Army Research Laboratory

A Study of Window Focusing Effects on Laser Ignition for Medium-Caliber Systems

by Jeffrey B. Morris and Richard A. Beyer

ARL-TR-2743 May 2002

Army Research Laboratory

Aberdeen Proving Ground, MD 21005-5066

ARL-TR-2743 May 2002

A Study of Window Focusing Effects on Laser Ignition for Medium-Caliber Systems

Jeffrey B. Morris and Richard A. Beyer
Weapons and Materials Research Directorate, ARL

Abstract

One proposed implementation of medium-caliber laser ignition employs a focusing ball to replace the conventional electric primer. The effects of ball size and igniter stand-off distance have been characterized experimentally with black powder pellets. Ignition threshold and delay experiments were carried out using 4-mm and 6-mm diameter glass beads with standoffs up to 1.5 mm. Ray tracing was used to model the energy distribution of a top-hat beam profile refracted through a focusing ball. Results of the study indicate that the tighter focus of the 4-mm bead can reduce the required laser pulse energy with little effect on the ignition delay.

Acknowledgments

This work was supported by the U.S. Army Environmental Quality Basic Research and Development (EQBRD) Program. The EQBRD program is managed through the Industrial Ecology Center at Picatinny Arsenal, NJ.

INTENTIONALLY LEFT BLANK.

Contents

INTENTIONALLY LEFT BLANK.

List of Figures

INTENTIONALLY LEFT BLANK.

List of Tables

INTENTIONALLY LEFT BLANK.

1. Introduction

In work described in a previous U.S. Army Research Laboratory (ARL) technical report, a 30-mm gun fixture was modified for laser ignition (Beyer and Hirlinger 1999). In that report several concepts for the modification of 30-mm ammunition to accept a laser ignition source were studied experimentally using single-round firings. Figure 1 depicts one of the more successful implementations where the electric primer has been replaced by a glass focusing ball in a housing, along with the addition of an ignition material specific for laser ignition and transfer to the flashtube.

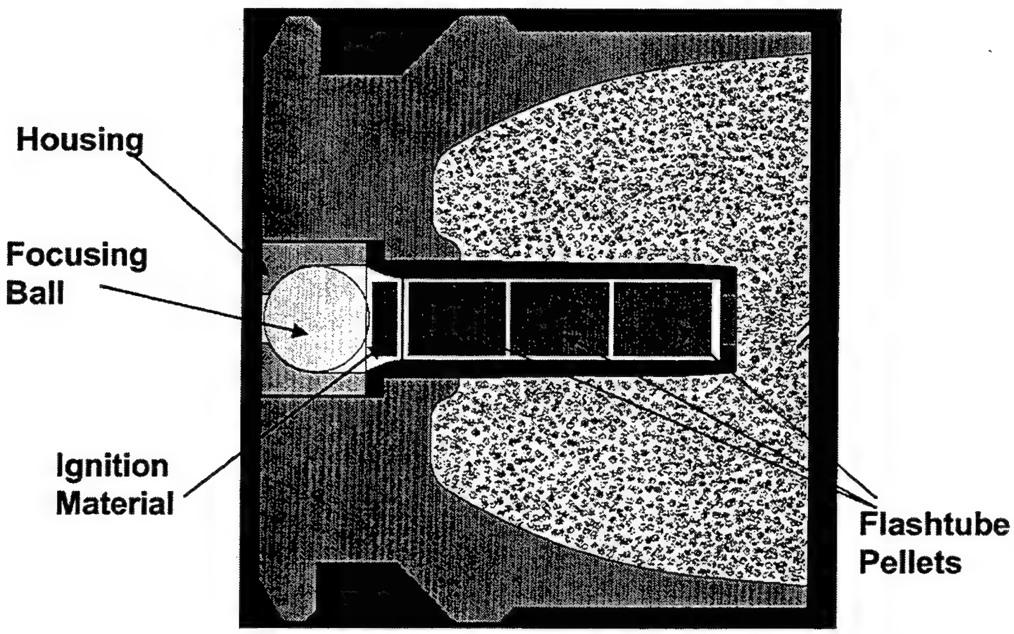

Figure 1. Ball window configuration for laser ignition of 30-mm ammunition.

In the configuration shown in Figure 1, the ignition material is pressed up against the focusing ball. We suspect that this configuration results in minimal focusing of the laser spot and that a smaller spot with greater intensity can be realized by incorporating a standoff between the focusing ball and the ignition material. The same effect might also be achieved through the use of a smaller-diameter ball. In this report we examine how stand-off distance and bead size affect the direct laser ignition of black powder pellets. While the direct ignition of black powder does not meet the action time* requirements (4 ms) for the 30-mm application, these pellets are a convenient sample for this fundamental laboratory study and should provide some additional insight into the initial ignition event.

*Action time is defined as the time from application of the firing pulse to the exit of the projectile from a gun barrel.

2. Experimental Setup

The experimental setup used for this study is shown in Figure 2. The output from a pulsed Nd^{3+} laser with a wavelength of 1.06 µm was truncated using an adjustable iris. The laser pulse length was set to 5 ms. The truncated beam was directed into a glass bead that was used as a short focal-length lens. A 100-mg black powder pellet was attached to a translation stage. The position of the black powder pellet was adjusted to provide various standoffs from the bead. Laser ignition experiments were carried out to determine the effect of the stand-off distance and bead diameter on the ignition threshold and time-to-first-light (TTFL). Two sets of bead/iris parameters were used. When using a 6-mm diameter bead, the laser beam diameter was truncated to 4.76 mm (3/16″). The experiments were also carried out using a 4-mm diameter bead with a truncated 3.18-mm (1/8″) beam diameter.

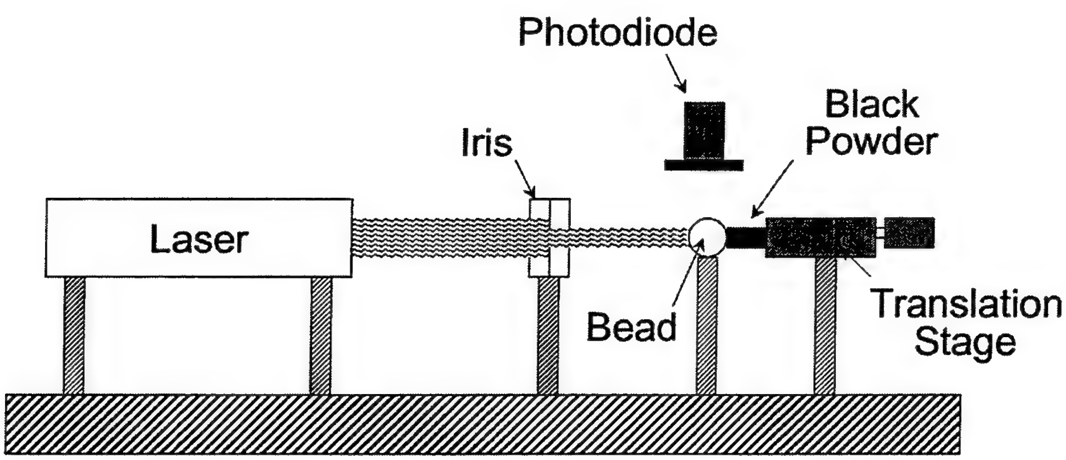

Figure 2. Experimental setup for the laser ignition experiment.

Ignition threshold data were measured in groups of three data points for each setting of laser lamp energy and stand-off distance. An energy meter placed between the iris and bead was used to measure laser pulse energy before each experiment. The three energy measurements were averaged for each set of experimental conditions. Go/No-Go data were based on the ignition of black powder pellet. A "Go Fraction" was determined as the number of Go events divided by the total number of experiments for a given set of conditions (in our case, 3).

The photodiode was used to generate time-to-first-light data. A transimpedance amplifier was used to convert current to voltage and the voltage trace was recorded using a digital oscilloscope. The oscilloscope was triggered using the leading edge of the laser pulse. A baseline light value was established for each

trace by averaging several milliseconds in the pretrigger region. TTFL was defined as the time for the photodiode trace to first exceed the baseline plus twice the resolution of the analog-to-digital (A/D) conversion in the oscilloscope. An average TTFL was calculated for each data set that had a Go Fraction of 1.

3. Experimental Data

Table 1 shows the experimental data for the experiments using a 6-mm diameter bead. Each line in the table represents an average of three individual experiments using a common set of conditions. The pulse energy, Go Fraction, and TTFL are averages for each data set. Table 2 shows the corresponding data for the 4-mm diameter bead.

Table 1. Experimental data for study using 6-mm diameter bead. Incident laser beam diameter = 4.76 mm.

Standoff (mm)	Pulse Energy (mJ)	Go Fraction	TTFL (ms)
0	788	1	10.4
0	477	1	9.8
0	345	1	11.5
0	170	1	15.9
0	94	1	15.8
0	87	1	18.9
0	81	0.67	–
0	73	0	–
0	69	0	–
0	70	0.33	–
0	62	0	–
0	58	0	–
0.5	59	1	21.6
0.5	26	1	27.5
0.5	22	0	–
0.5	14	0	–
1.0	27	1	30.1
1.0	13	1	31.9
1.0	10	0	–
1.0	5.3	0	–
1.0	2.1	0	–
1.5	17	1	33.4
1.5	13	0.33	–
1.5	12	0.66	–
1.5	9.1	0	–

Table 2. Experimental data for study using 4-mm diameter bead. Incident laser beam diameter = 3.18 mm.

Standoff (mm)	Pulse Energy (mJ)	Go Fraction	TTFL (ms)
0	192	1	14.7
0	115	1	11.5
0	44	1	19.9
0	29	0.33	—
0	25	0.33	—
0	11	0.0	—
0.5	23	1	26.7
0.5	14	1	27.9
0.5	9.7	1	28.6
0.5	7.4	0.67	—
0.5	6.5	0.33	—
0.5	4.6	0	—
1.0	12	1	27.6
1.0	10	1	32.0
1.0	9.7	0.67	—
1.0	7.2	0.67	—
1.0	5.7	0.67	—
1.0	4.6	0	—

4. Spot Size and Spatial Energy Distribution

As part of a Phase I Small Business Innovative Research (SBIR) contract (DAAD17-01-C-0061), Aurora Optics carried out preliminary ray tracing on the 6-mm focusing ball and determined a focal length of 1.4 mm (Burke 2001). In order to further investigate the refraction of a non-divergent beam with a top-hat profile through a sphere, we devised and implemented a ray-tracing model using the Microsoft Excel spreadsheet. For this model, the refractive index of air was taken to be 1.00 and the refractive index of the glass bead was taken to be 1.51 for a laser wavelength of 1.064 μm. The top-hat assumption is reasonable when one considers that an iris truncated the beam. Removing the wings from a Gaussian beam results in a much smaller variation in energy distribution across the cross-section of the resultant spot. Ray tracing was used to establish spot sizes and energy profiles for the 6-mm bead at various stand-off distances up to 1.5 mm beyond the bead. Only spot sizes were calculated for the 4-mm bead.

Spot sizes were calculated using five sets of rays corresponding to the 20%, 40%, 60%, 80%, and 100% energy contours across the spot size of the laser beam incident to the glass bead. Figure 3 shows the mapping of equal-area regions to radial ray positions. Figure 4 shows the refraction of these rays through a 6-mm diameter glass bead. Spot diameters were determined from the radial position of

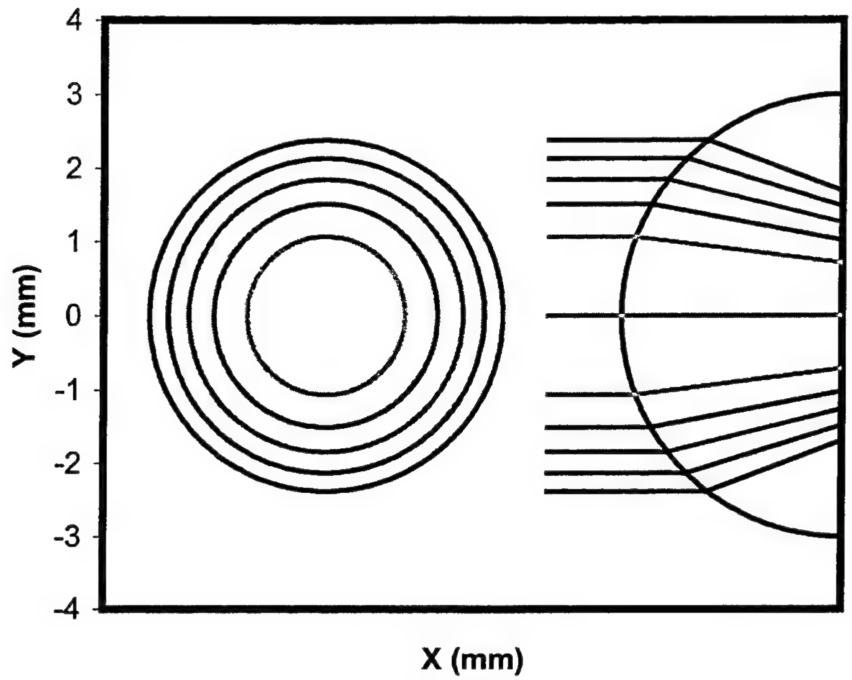

Figure 3. Mapping of 20% areal contours for a top-hat energy distribution (left) to ray projections (right).

the ray furthest from the beam centerline at each stand-off distance beyond the bead. The outermost ray at each standoff defines the boundary that contains 100% of the refracted energy. Tables 3 and 4 list the spot sizes as a function of standoff for the 6-mm and 4-mm bead, respectively.

The calculated diameters only define the boundaries of the spot, but yield no information regarding the distribution of energy. Spatial energy distributions were calculated for the case of the 6-mm diameter bead by repeating the ray-tracing procedure for 100 rays corresponding to equal-area annular regions. Each ray corresponds to a 1% energy contour using a top-hat spatial profile for the incident laser beam. The position of each ray was calculated through the glass bead at specific stand-off distances. A density-of-rays approach was employed to determine the energy distribution beyond the glass bead using an assumption that each ray corresponded to 1% of the total energy in the spot at each standoff. A minimum thickness of 10 μm was used when counting the rays in each annular area. Figure 5 shows the calculated energy distribution at 4 standoff distances used for the 6-mm bead plotted as peak laser intensity for a 5-ms, 100-mJ pulse. These calculations indicate enhanced perimeter laser intensity for standoffs at 0.0 mm and 0.5 mm. The energy distribution for standoffs of 1.0 and 1.5 mm indicate enhanced intensity at the middle of the spot.

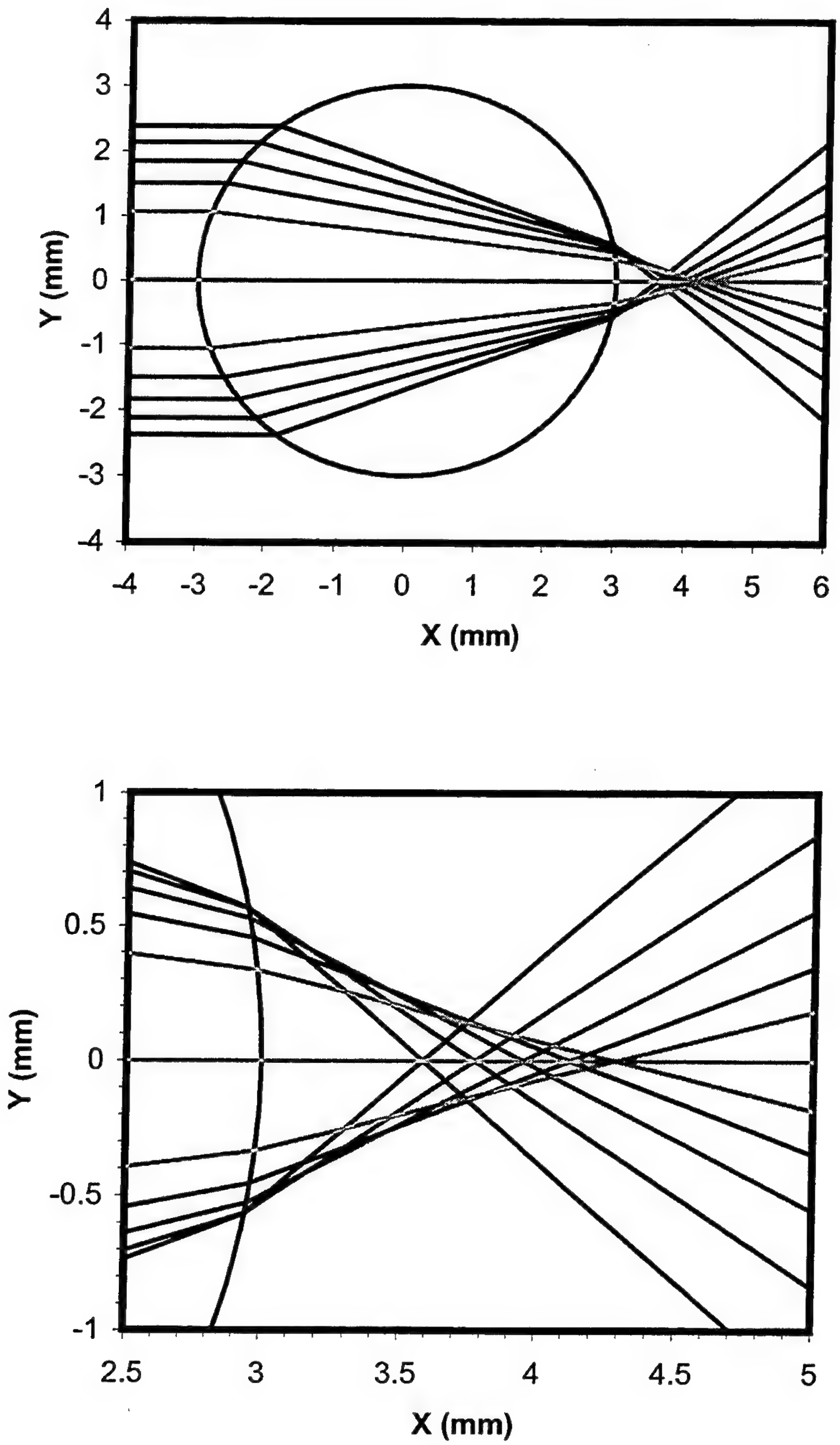

Figure 4. Refraction of 4.76-mm diameter beam passing through 6-mm diameter glass bead.

Table 3. Spot size as a function of standoff behind a 6-mm diameter glass bead for a 4.76-mm diameter incident laser beam.

Position (mm)	Standoff (mm)	Spot Radius (mm)	Spot Area (cm^2)
3.0	0.0	0.53	0.00877
3.5	0.5	0.25	0.00187
3.7*	0.7	0.16	0.00086
4.0	1.0	0.37	0.00431
4.5	1.5	0.81	0.02087

*Beam Waist

Table 4. Spot size as a function of standoff behind a 4-mm diameter glass bead for a 3.18-mm diameter incident laser beam.

Position (mm)	Standoff (mm)	Spot Diameter (mm)	Spot Area (cm^2)
2.0	0.0	0.70	0.00390
2.5*	0.5	0.20	0.00031
3.0	1.0	1.09	0.00931

*Beam Waist

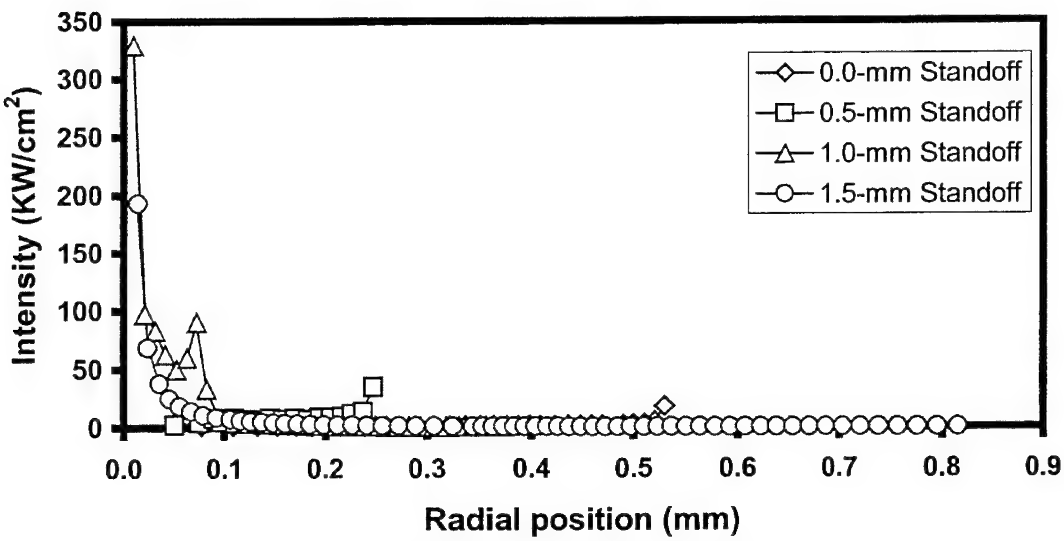

Figure 5. Intensity distribution calculated as a function of stand-off distance behind a 6-mm glass bead for a 5-ms, 100-mJ laser pulse.

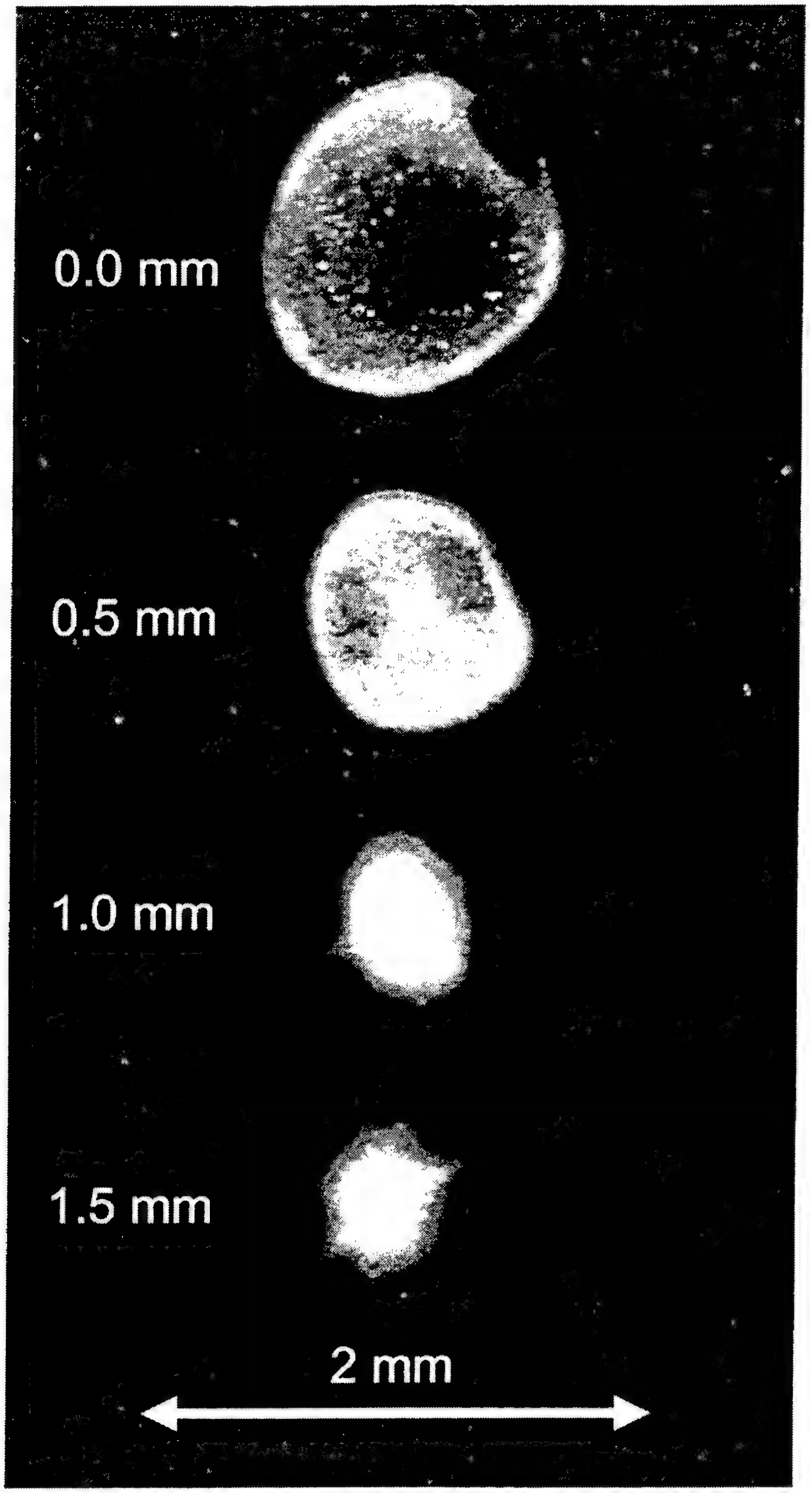

Figure 6. Laser spot imaging on burn paper at bead exit stand-off distances of 0.0-, 0.5-, 1.0-, and 1.5-mm for a 6-mm diameter bead with 4.76-mm incident beam diameter, 5-ms pulse length, and 15-mJ average incident laser pulse energy.

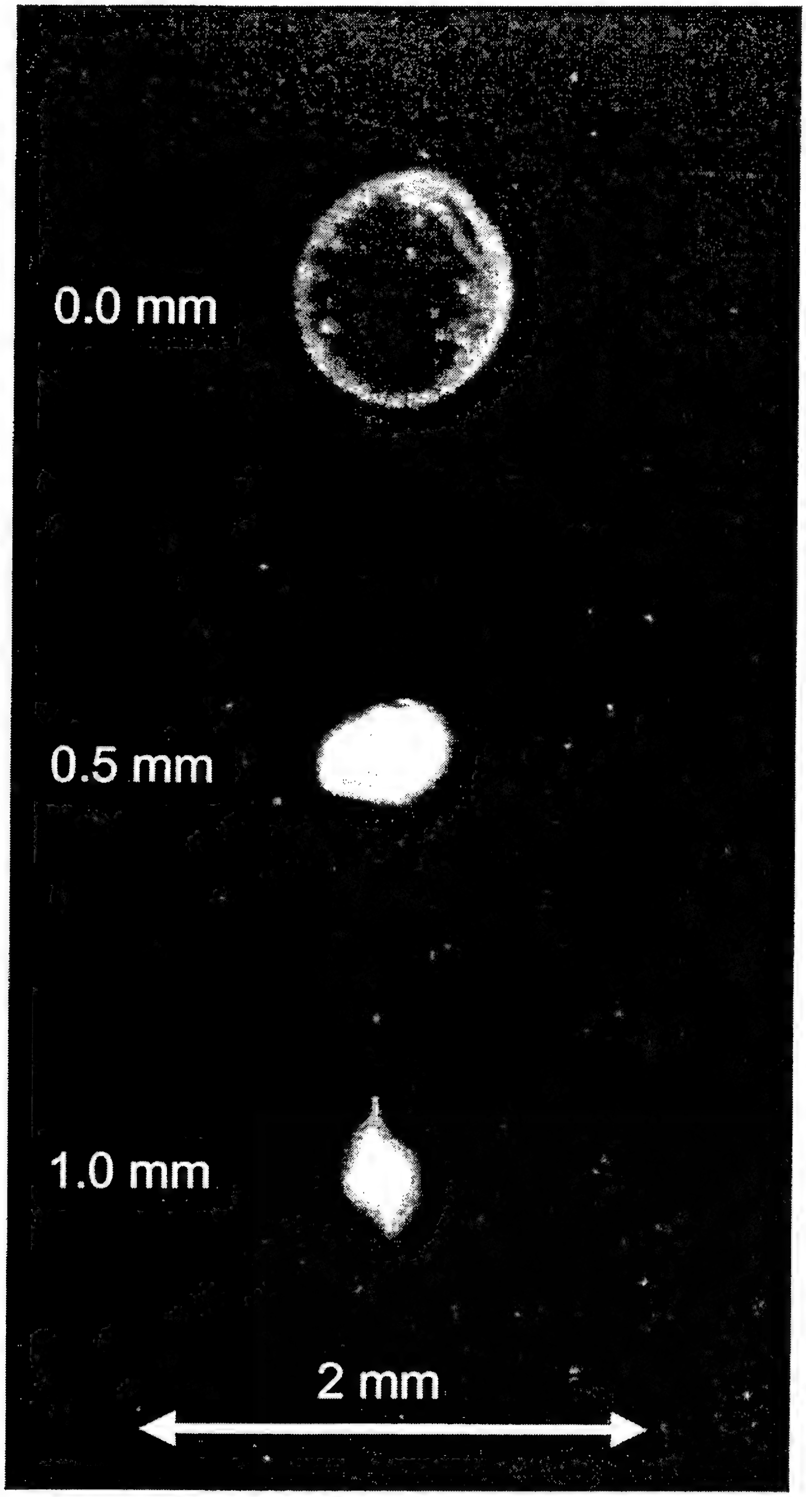

Figure 7. Laser spot imaging on burn paper at bead exit stand-off distances of 0.0-, 0.5-, and 1.0-mm for a 4-mm diameter bead with 3.18-mm incident beam diameter, 5-ms pulse length, and 12-mJ average incident laser pulse energy.

Additional ray-tracing analysis shows that the individual rays come to a focus (i.e., cross the center line of the bead) at stand-off distances of 0.58 to 1.44 mm, with the rays originally at the perimeter of the incident beam being most strongly refracted and coming to a focus first. Our focus calculations are in excellent agreement with the Aurora Optics results, which were modeled using a smaller 2.5 mm diameter beam. At stand-off distances of 0.0 and 0.5 mm, none of the individual rays have yet come to a focus, hence the appearance of the ring intensification pattern in the energy distribution. The standoff of 1.0 mm is near the center of this focusing region and displays a very large intensity near the center of the spot. The standoff at 1.5 mm is just beyond the focusing region.

For these last two standoffs, the majority of the energy is localized in a much smaller spot than those predicted in Table 3. Referring to Figure 4, for standoffs beyond the beam waist, it is evident that the ray that corresponds to the original 100% contour defines gross spot size. Having come to a focus close to the bead, this ray will diverge with a larger angle than those rays closer to the center of the beam that come to a focus further out. At the distance where the innermost rays come to a focus, the highly divergent rays distribute their energy over a large area, resulting in a large spot size with a fairly low intensity in the perimeter, but with a high intensity in the center where other rays are focused—or diverging much slower—in a small area.

To validate the predicted tendencies, the experiments depicted in Figure 2 were repeated using laser burn paper in place of the black powder pellet. Burn patterns are presented in Figures 6 and 7 for 6-mm and 4-mm beads, respectively. Both figures show a ring pattern at 0-mm standoff with the intense portion of the spot burning smaller areas at the larger standoffs. Figure 6 can be compared directly with Figure 4. The more detailed ray tracing was not done for the 4-mm bead. The beam diameter was scaled down in proportion to the bead size relative to the parameters used for the 6-mm bead—both were reduced by 33%. Thus, the spot sizes and energy distributions would scale down by 33% at standoffs scaled down by the same factor.

5. Discussion

Two important issues for laser ignition are ignition delay and threshold energy. Ignition delay can be especially critical for a system such as the 30-mm M230 chain gun, whose ballistic cycle allows only a very short time in battery. The threshold energy requirement affects the volume and weight of the laser package required for effective ignition.

Figure 8 shows a plot of "Go Fraction" vs. total laser pulse energy incident to the 6-mm glass bead. The data show the lowest energy thresholds for laser ignition of black powder occur at stand-off distances of 1.0 to 1.5 mm. Figure 9 shows similar data for the experiments using the 4-mm bead. For these data, the lowest energy thresholds occur at stand-off distances of 0.5 to 1.0 mm. Comparison of Figures 8 and 9 show laser ignition thresholds for the 4-mm bead to be substantially lower than those observed for the 6-mm bead at similar stand-off distances (see also Tables 1 and 2). At 0-mm standoff, the ignition threshold energy using the 4-mm bead is half that for the 6-mm bead. The tighter focus of the 4-mm bead results in smaller spot sizes with greater intensity relative to the 6-mm bead. The results of this effect can be seen in the burn patterns shown in Figures 6 and 7.

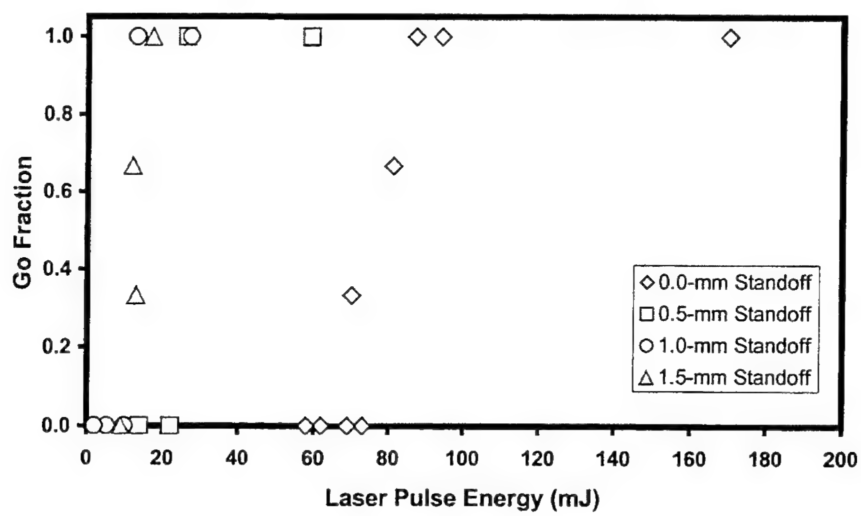

Figure 8. Plot of Go Fraction vs. total incident laser pulse energy for 6-mm bead, 4.76-mm beam diameter.

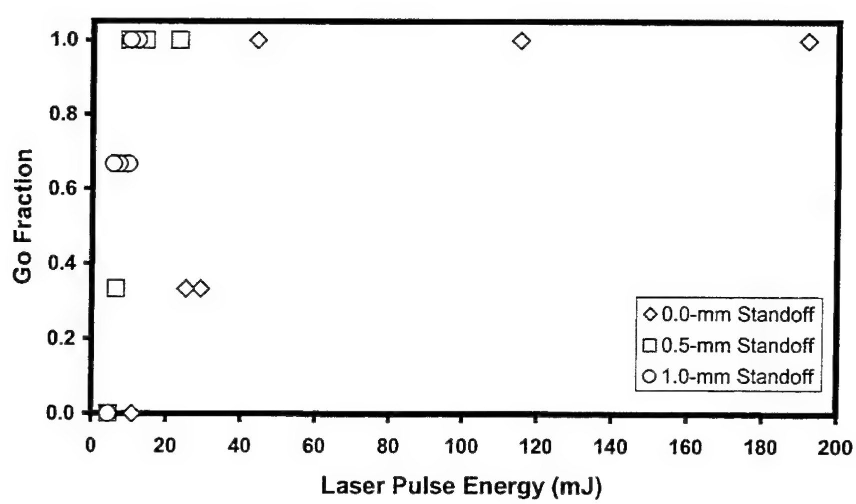

Figure 9. Plot of Go Fraction vs. total incident laser pulse energy for 4-mm bead, 3.18-mm beam diameter.

Ignition delay is characterized by TTFL. A tradeoff exists between energy threshold and ignition delay. At low-laser intensities, energy absorption, melting, and heat transfer govern the ignition event. As the laser intensity is increased, eventually the incident energy flux exceeds the capacity for absorption and heat transfer, and the excess energy is converted into kinetic energy through ablation of the target material. In experiments where a laser beam with a top-hat profile and a fixed spot size is used to ignite a propellant, one typically observes large ignition delays near ignition threshold, with shorter delays as the intensity is increased until ablation becomes significant. The ignition delay increases at higher ablative laser intensities. Given enough information about the propellant system, it is possible to model the ignition delay as a function of the energy flux, at least in the pre-ablative region (Cohen and Beyer 1993).

As a first approximation one could convert the pulse energies (mJ) listed in Tables 1 and 2 into intensity (KW/cm^2) using the 5-ms pulse width and the gross spot areas listed in Tables 3 and 4. However, the data presented in Figures 5, 6, and 7 reveal very nonuniform energy distributions once the laser pulse has been refracted by the focusing ball. We observe two different types of energy distributions as a function of stand-off distance. At short standoff, much of the energy is concentrated in a ring at the spot perimeter. At long standoff, a majority of the energy is focused in a spot that is much smaller than the gross spot areas indicated in Tables 3 and 4. While some shot-to-shot variation in the laser pulse energy is observed, the burn patterns presented in Figures 6 and 7 are repeatable.

Due to the large variation in the laser intensity distribution patterns at different stand-off distances, there is no meaningful way to plot ignition delay vs. laser intensity. As an alternate presentation, Figures 10 and 11 show plots of TTFL vs. laser energy incident to the glass bead. We note that the average TTFL values at ignition threshold are similar for the two data sets at similar standoffs: 19–20 ms at 0 mm, 27–29 ms at 0.5 mm, and 32 ms at 1.0 mm. The similar ignition delays would indicate similar ignition threshold laser intensities. With the tighter focus of the 4-mm bead, it is possible to achieve similar laser intensity using less incident energy than would be required for the 6-mm bead and without a significant change in ignition delay.

6. Conclusions

The objectives of this study were to determine the potential benefit to medium-caliber laser ignition by incorporating a standoff between the focusing ball and the material being ignited. In addition, we also investigated the differences between using a 6-mm and 4-mm diameter focusing ball. The experiments were limited to black powder pellets. Our conclusions are summarized as follows:

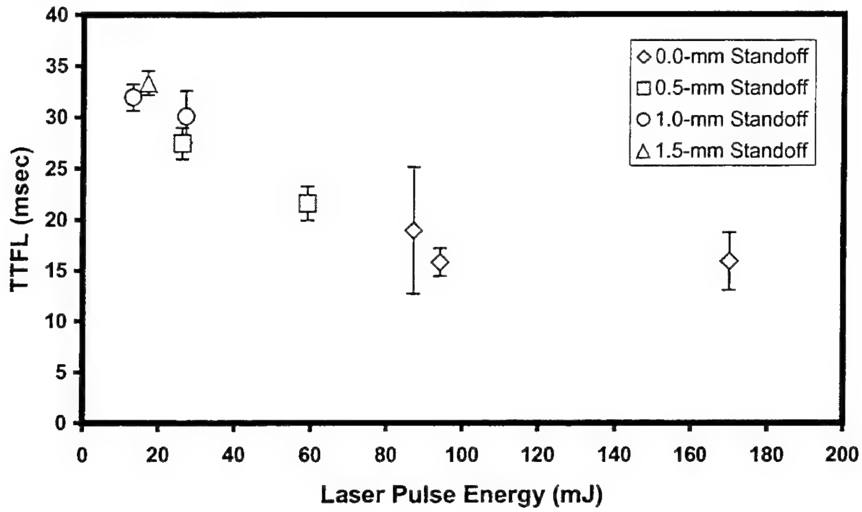

Figure 10. Time-to-first-light vs. estimated laser pulse energy for the ignition of black powder using a 6-mm diameter bead lens and a 4.76-mm diameter laser beam.

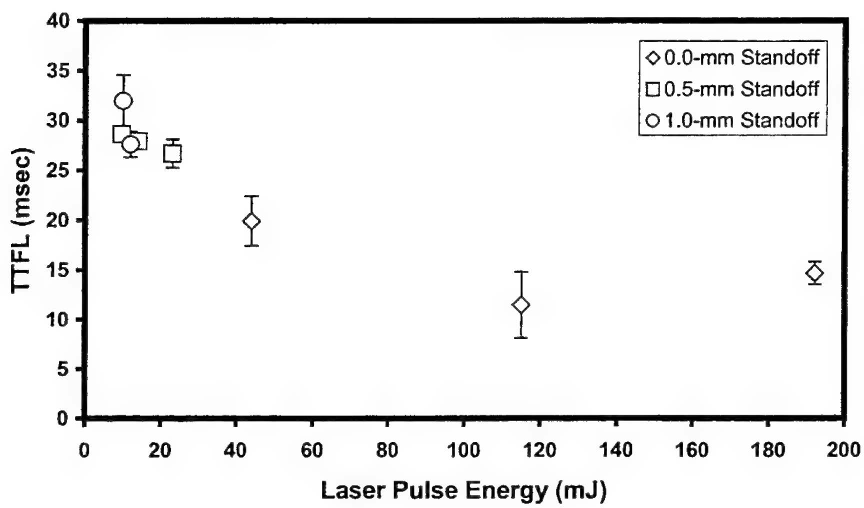

Figure 11. Time-to-first-light vs. estimated laser pulse energy for the ignition of black powder using a 4-mm diameter bead lens and a 3.18-mm diameter laser beam.

- A laser pulse with a top-hat energy distribution refracting through a glass ball will have a nonuniform energy distribution that changes dramatically as a function of stand-off distance from the ball. At a short stand-off distance, much of the energy is concentrated in a ring at the perimeter of the spot. At longer standoffs, the majority of the energy is concentrated in a much smaller spot.
- Ignition threshold energy decreases as standoff is increased in the range of 0 to 1.5 mm.

- Ignition delay at threshold increases as standoff is increased in the range of 0 to 1.5 mm.
- With the tighter focus of the 4-mm bead, it is possible to achieve similar ignition delays at threshold using less incident energy than would be required for the 6-mm bead.

We also note that the minimum ignition delays for both sets of data using the 4-mm and 6-mm beads were minimized at 0-mm standoff, using a pulse-energy substantially greater than the ignition threshold. However, experiments at standoff distances greater than 0 mm were carried out only at pulse energies near ignition threshold. It is likely that increased pulse energies at nonzero standoffs would result in reduced ignition delays. We cannot conclude that the minimum ignition delay at 0 mm is a global minimum for all standoffs or that a similar ignition delay requiring less energy could not be achieved at a nonzero standoff.

Recommendations:

- Due to its tighter focus and lower energy thresholds, the smaller 4-mm focusing ball should be implemented.
- The efficacy of this new configuration should be validated through additional firings using a Mann barrel.

The decrease in energy threshold can result in the implementation of a laser system with less volume and mass. A smaller system would positively impact engineering efforts to retrofit a laser ignition source to an existing gun system.

7. References

Beyer, R. A., and J. M. Hirlinger. "Laser Ignition in a Medium-Caliber Gun: A Study of Igniter Influence on Action Time." ARL-TR-1864, U.S. Army Research Laboratory, Aberdeen Proving Ground, MD, January 1999.

Burke, G. Personal communication. Aurora Optics Inc., Hanover, NH, September 2001.

Cohen, A., and R. A. Beyer. "Laser Ignition of Solid Propellants: I. Ignition Delays." ARL-TR-162, U.S. Army Research Laboratory, Aberdeen Proving Ground, MD, July 1993.

INTENTIONALLY LEFT BLANK.

NO. OF COPIES	ORGANIZATION
2	DEFENSE TECHNICAL INFORMATION CENTER DTIC OCA 8725 JOHN J KINGMAN RD STE 0944 FT BELVOIR VA 22060-6218
1	HQDA DAMO FDT 400 ARMY PENTAGON WASHINGTON DC 20310-0460
1	OSD OUSD(A&T)/ODDR&E(R) DR R J TREW 3800 DEFENSE PENTAGON WASHINGTON DC 20301-3800
1	COMMANDING GENERAL US ARMY MATERIEL CMD AMCRDA TF 5001 EISENHOWER AVE ALEXANDRIA VA 22333-0001
1	INST FOR ADVNCD TCHNLGY THE UNIV OF TEXAS AT AUSTIN 3925 W BRAKER LN STE 400 AUSTIN TX 78759-5316
1	US MILITARY ACADEMY MATH SCI CTR EXCELLENCE MADN MATH THAYER HALL WEST POINT NY 10996-1786
1	DIRECTOR US ARMY RESEARCH LAB AMSRL D DR D SMITH 2800 POWDER MILL RD ADELPHI MD 20783-1197
1	DIRECTOR US ARMY RESEARCH LAB AMSRL CI AI R 2800 POWDER MILL RD ADELPHI MD 20783-1197

NO. OF COPIES	ORGANIZATION
3	DIRECTOR US ARMY RESEARCH LAB AMSRL CI LL 2800 POWDER MILL RD ADELPHI MD 20783-1197
3	DIRECTOR US ARMY RESEARCH LAB AMSRL CI IS T 2800 POWDER MILL RD ADELPHI MD 20783-1197

ABERDEEN PROVING GROUND

2	DIR USARL AMSRL CI LP (BLDG 305)

NO. OF COPIES	ORGANIZATION
	ABERDEEN PROVING GROUND
31	DIR USARL AMSRL WM BD W R ANDERSON R A BEYER A BIRK A L BRANT S W BUNTE C F CHABALOWSKI L M CHANG T P COFFEE J COLBURN P J CONROY R A FIFER B E FORCH B E HOMAN S L HOWARD P J KASTE A J KOTLAR C LEVERITT K L MCNESBY M MCQUAID M S MILLER T C MINOR A W MIZIOLEK J B MORRIS J A NEWBERRY M J NUSCA R A PESCE-RODRIGUEZ G P REEVES B M RICE R C SAUSA J A VANDERHOFF A W WILLIAMS

NO. OF COPIES	ORGANIZATION
1	PROGRAM EXECUTIVE OFFICE AVIATION BLDG 5681 WOODS RD REDSTONE ARSENAL AL 35898
1	PM APACHE N BRUCHMAN REDSTONE ARSENAL AL 35898
1	COMMANDER TACOM ARDEC AMSTA AR CCL B W BUNTING PICATINNY ARSENAL NJ 07806-5000
3	COMMANDER TACOM ARDEC AMSTA AR CCL C J HIRLINGER PICATINNY ARSENAL NJ 07806-5000
1	COMMANDER TACOM ARDEC AMSTA AR CCL D J GUELPH PICATINNY ARSENAL NJ 07806-5000
1	COMMANDER TACOM ARDEC AMSTA AR WEE T DORIS JR PICATINNY ARSENAL NJ 07806-5000
2	COMMANDER TACOM ARDEC AMSTA AR WET T SACHAR D TOLLIVER PICATINNY ARSENAL NJ 07806-5000
1	MEGAWATT LASERS 18 HUNTER RD, SUITE 6 S HAMLIN HILTON HEAD ISLAND SC 29926

NO. OF COPIES	ORGANIZATION
1	AURORA OPTICS INC PO BOX 493 G BURKE HANOVER NH 03755
2	CDR USAATC STEAC TS PC P MARSH A RAUNIG BLDG 363 APG MD 21005-5059
7	DIR USARL AMSRL WM B A HORST AMSRL WM M J PLUMER AMSRL WM MC R ADLER AMSRL WM TB P BAKER R SKAGGS L VANDE KIEFT W HILLSTROM

INTENTIONALLY LEFT BLANK.

REPORT DOCUMENTATION PAGE

Form Approved
OMB No. 0704-0188

1. AGENCY USE ONLY *(Leave blank)*	2. REPORT DATE	3. REPORT TYPE AND DATES COVERED
	May 2002	Final, October 2001 – March 2002

4. TITLE AND SUBTITLE
A Study of Window Focusing Effects on Laser Ignition for Medium-Caliber Systems

5. FUNDING NUMBERS
611102.H67

6. AUTHOR(S)
Jeffrey B. Morris and Richard A. Beyer

7. PERFORMING ORGANIZATION NAME(S) AND ADDRESS(ES)
U.S. Army Research Laboratory
ATTN: AMSRL-WM-BC
Aberdeen Proving Ground, MD 21005-5066

8. PERFORMING ORGANIZATION REPORT NUMBER
ARL-TR-2743

9. SPONSORING/MONITORING AGENCY NAMES(S) AND ADDRESS(ES)
TACOM-ARDEC
ATTN: AMST-AR-WET
Picatinny Arsenal, NJ 07806-5000

10.SPONSORING/MONITORING AGENCY REPORT NUMBER

11. SUPPLEMENTARY NOTES

12a. DISTRIBUTION/AVAILABILITY STATEMENT
Approved for public release; distribution is unlimited.

12b. DISTRIBUTION CODE

13. ABSTRACT*(Maximum 200 words)*

One proposed implementation of medium-caliber laser ignition employs a focusing ball to replace the conventional electric primer. The effects of ball size and igniter stand-off distance have been characterized experimentally with black powder pellets. Ignition threshold and delay experiments were carried out using 4-mm and 6-mm diameter glass beads with standoffs up to 1.5 mm. Ray tracing was used to model the energy distribution of a top-hat beam profile refracted through a focusing ball. Results of the study indicate that the tighter focus of the 4-mm bead can reduce the required laser pulse energy with little effect on the ignition delay.

14. SUBJECT TERMS	15. NUMBER OF PAGES
laser ignition, black powder, medium-caliber gun	25
	16. PRICE CODE

17. SECURITY CLASSIFICATION OF REPORT	18. SECURITY CLASSIFICATION OF THIS PAGE	19. SECURITY CLASSIFICATION OF ABSTRACT	20. LIMITATION OF ABSTRACT
UNCLASSIFIED	UNCLASSIFIED	UNCLASSIFIED	UL

NSN 7540-01-280-5500

Standard Form 298 (Rev. 2-89)
Prescribed by ANSI Std. 239-18 298-102

INTENTIONALLY LEFT BLANK.